

## RESEARCH ARTICLE

# Machine Learning Based Prediction of Reference Evapotranspiration ( $ET_0$ ) Using IoT

ZHIMING HU<sup>1</sup>, RAB NAWAZ BASHIR<sup>1,2</sup>, AQEEL UR REHMAN<sup>2</sup>, SALMAN IQBAL<sup>2</sup>,  
MALIK MUHAMMAD ALI SHAHID<sup>1,2</sup>, AND TING XU<sup>3</sup>

<sup>1</sup>Consumer Protection Department, Hubei Supervision Bureau of China Banking and Insurance Regulatory Commission, Wuhan, Hubei 430000, China

<sup>2</sup>Department of Computer Science, COMSATS University Islamabad, Vehari 61100, Pakistan

<sup>3</sup>Department of Economics and Management, Wenhua College, Hubei 430000, China

Corresponding author: Rab Nawaz Bashir (rabnawaz@cuivehari.edu.pk)

**ABSTRACT** Accurate estimation of Reference Evapotranspiration ( $ET_0$ ) is important for efficient management and conservation of irrigation water. Existing methods of  $ET_0$  rate determination are complex for application at the farmer level. Apart from standard methods of  $ET_0$  determination, many data-driven soft computing approaches were also proposed to determine the  $ET_0$  with limited data set. We proposed a temperature and humidity-based ML approach for  $ET_0$  rate determination on directly sensed environmental conditions of the crop field. Crop field environmental conditions for ( $ET_0$ ) rate determination are sensed by the proposed Internet of Things (IoT) architecture. Crop field environmental conditions from the year 2015 to 2021 in Pakistan are used for the training and testing of the proposed model. Gaussian Naive Bayes (GNB), Support Vector Machine (SVM), k-Nearest Neighbours (KNN), and Artificial Neural Network (ANN) based models are compared for performance. Crop fields directly sensed temperature and humidity pass to the model to train and predict the  $ET_0$ -rate of crop fields. The 10-fold cross-validation technique is applied for the evaluation of the proposed approach. The accuracy of the proposed solution for the  $ET_0$  rate is compared against the Food and Agriculture Organization (FAO) recommended Penman-Monteith method for  $ET_0$  rate determination. As concerned of the ML-based models the KNN model is more accurate as compared to SVM, GNB and ANN models with 92% accuracy. The KNN model of  $ET_0$  is more efficient in reducing the Root Mean Squared Errors (RMSE) by 16% and Mean Absolute Errors (MAE) by 3% against the state of the art approach.

**INDEX TERMS** Internet of Things (IoT), reference evapotranspiration ( $ET_0$ ), support vector machine (SVM), Gaussian Naive Bayes (GNB), K-nearest neighbour (KNN), artificial neural network (ANN), Penman-Monteith.

## I. INTRODUCTION

Agriculture is the source of major necessities of life for human beings. 60% of irrigation waters used for irrigation purposes is wasted due to poor agronomic activities [1]. In recent years, the agriculture sector has been suffering from many challenges to feed the ever-increasing human population [2]. Low productivity, urbanization, shortage of fresh irrigation water, and land degradation are the significant issues of agriculture across the world [3]. Agriculture is under immense pressure to improve productivity, to feed the

ever-increasing human population, that would be six billion in 2050. To improve agriculture productivity efficient management of irrigation water is important to support sustainable developments. The application of irrigation water according to the  $ET_0$  rate is the foundation of irrigation water conservation.  $ET_0$  is the major element of the hydrological cycle and foundation of irrigation water planning [4], [5].  $ET_0$  is the key element of water resource management for the improvement in water productivity [6].  $ET_0$  accounts for more than one-third of the global precipitation losses [7].  $ET_0$  adjusts the irrigation according to the prevailing petrological conditions while maintaining the yield. Spatio-temporal distribution of  $ET_0$  is the key to irrigation water management [6], [7].

The associate editor coordinating the review of this manuscript and approving it for publication was Liang-Bi Chen<sup>1</sup>.

Therefore, the  $ET_0$  rate is a very important part of irrigation water scheduling [8].  $ET_0$  is an important part of irrigation water management [7]. Efficient irrigation water management is important to support the conservation of irrigation water by  $ET_0$  rate while maintaining yield.  $ET_0$  is the measure of water loss from the earth and plant surface.  $ET_0$  adjusts the amount of irrigation water according to the meteorological conditions.  $ET_0$  is the most important issue in water resource management and planning [9]. Irrigation water schedule according to the  $ET_0$  rate supports the conservation of irrigation water while maintaining yield [10].  $ET_0$  is important for efficient irrigation water scheduling for effective irrigation water utilization [5]. There are different methods for  $ET_0$  measurements like field measurements, experiment methods, and mathematical equations, measurements like meteorological data named, Blaney Criddle, Pan Evaporation, and Penman-Monteith methods [7]. These models are well accepted by agriculture communities but required a lot of meteorological data [7]. In general, these models require temperature, humidity, wind speed, solar radiation, the slope of vapor pressure, altitude, latitude, and rainfall for accurate calculation of the  $ET_0$  rate of a location. Applications of these models are complex and are unsuitable for application at the farmers' level for irrigation water scheduling [7].  $ET_0$  estimation with limited meteorological conditions is important for the successful implementation of the  $ET_0$  in precision irrigation applications. Determination of  $ET_0$  from limited environmental conditions is important for the implementation purpose. Moreover, the accurate prediction of the  $ET_0$  is also equally important. Therefore, the proposed solution aims to determine the  $ET_0$  rate according to the prevailing crop field by directly sensing the environment conditions from crop field. The IoT-assisted crop field environmental condition sensing is important for accurate predictions of the  $ET_0$  rate. Therefore the proposed solution aims to determine the accurate  $ET_0$  from limited environmental conditions by directly sensing of crop fields.

To simplify the  $ET_0$  rate determination many ML based solutions were proposed to estimate the  $ET_0$  rate with limited meteorological conditions. ML has emerged as a powerful tool for modeling  $ET_0$  with limited meteorological conditions [11], [12] [13]. Apart from these models modern Information and Communication Technologies (ICT) are extensively used for Precision Agriculture (PA) applications. Internet of Things (IoT) and ML are extensively used in agriculture to deal with long-lasting problems. IoT has shown significant success in many areas of life like smart cities, smart homes, smart health care, and agriculture is no exception [14] as shown in Fig. 1. IoT is the foundation of Precision Irrigation (PI) and smart irrigation applications. IoT is a new paradigm that enables the integration of the sensor into the application environment to capture the context of services and to adjust the services according to the context. IoT is a strong candidate to deal with long-lasting problems in agriculture due to its ability to capture context from remote agriculture fields, at a low cost. IoT can

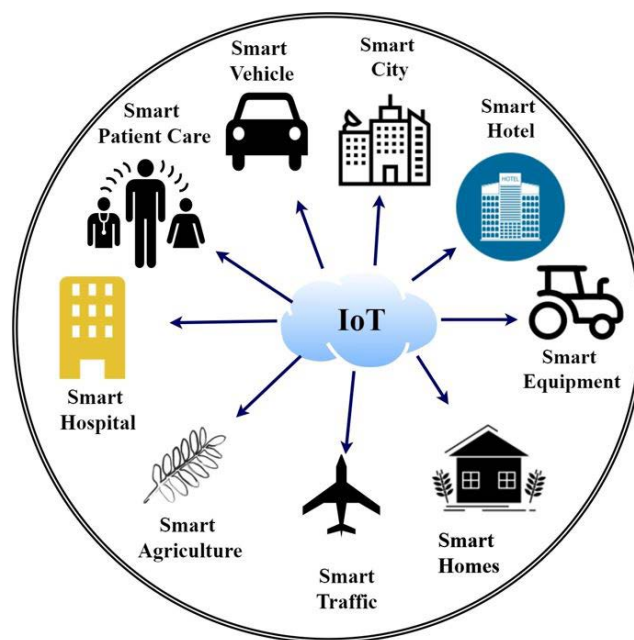


FIGURE 1. IoT applications.

directly sense parameters from the farmer field to provide useful information to the farmers for appropriate resource use and improve agricultural practices. IoT has the potential to capture the farming data directly from the crop field to determine the  $ET_0$  rate accordingly [15]. Many IoT-assisted solutions were proposed in agriculture focusing on monitoring and controlling the crop field area, precision irrigation management, and yield calibrations. In agriculture smart and Precision Irrigation (PI), applications are extensively used by sensing the crop field environments. Most IoT-based smart irrigation water solutions are based on sensing environmental and soil moisture conditions. The existing IoT-based smart irrigation water solution is usually based on soil moisture conditions and ignores the adjustments of irrigation water according to the  $ET_0$ , due to the complexity associated with  $ET_0$  determination.

To simplify the  $ET_0$  rate determinations, many ML-assisted solutions were proposed in recent years. The solutions attempt to determine the  $ET_0$  rate with limited meteorological conditions with reasonable accuracy [15]. Different studies and solutions address the problem of  $ET_0$  rate determination in different areas of the world. Due to the inherent complexity of the process efforts were made to develop different models for different regions of the world. China, India, and America are areas where the problem is addressed in many ways. These approaches use the meteorological conditions of weather stations rather than crop field environmental conditions. The use of crop field environmental conditions would calibrate the  $ET_0$  rate according to the crop field and would truly represent irrigation water estimation. The IoT-assisted directly sensed crop field environmental conditions can improve the accuracy

of the  $ET_0$  rate and would be a true reflection of the crop field conditions.

From this perspective, this paper proposes a machine learning approach for  $ET_0$ -rate determination to overcome the complexity associated with standard  $ET_0$ -rate determination methods. It captures the temperature and humidity of a crop field using IoT devices. The directly sensed temperature and humidity are passed into ML models for training, testing, and validation of the proposed solution. To evaluate the proposed approach, 10-fold cross-validation technique is applied. The significant contributions and unique features of the proposed solutions are as follows:

- A machine learning approach is proposed for  $ET_0$ -rate determination with temperature and humidity only to overcome the complexity associated with standard  $ET_0$ -rate determination.
- The proposed approach is based on  $ET_0$  rate determination from directly sensed crop field environment conditions.
- IoT architecture is proposed for the sensing of the real-time crop field environmental conditions to accurately estimate the  $ET_0$ -rate according to the prevailing crop field environmental conditions.
- The proposed solution estimate  $ET_0$  by FAO recommended Penman-Monteith  $ET_0$  rate determination method. The estimated  $ET_0$  would be acceptable for agriculture communities. The estimated  $ET_0$  by the proposed solution is compared against the Penman-Monteith method.
- The study also compares the performance of the different ML models in the determination of the  $ET_0$  rate from directly sensed crop field environmental conditions.

## II. RELATED WORK

Accurate estimation of  $ET_0$  is important for precise irrigation water requirements and irrigation water resources management [14].  $ET_0$  rate estimation is most important in irrigation water scheduling [11]. Due to the importance of the problem many solutions were emerged in recent years regarding irrigation water recommendations according to prevailing environmental conditions using modern sensing and communication technologies like IoT. Many efforts were also made regarding the estimation of  $ET_0$  from limited meteorological conditions. Renowned bibliographic indices are searched to find the related work regarding precision irrigation, smart irrigation, and  $ET_0$  rate determination.

Ferreira L *et al.* proposed monthly  $ET_0$  estimation using Random Forest (RF), ANN, Xboost, and Convolution Neural Network (CNN) from hourly conditions. The results of the study indicate that CNN models are accurate with RMSE reduced up to 28% [11]. Yemac Sevin Seda and Todorovic Mladen proposed crop potential Evapotranspiration ( $ET_c$ ) using the Artificial Neural Network (ANN) and K-Nearest Neighbour (KNN) models [16]. Chen Z. *et al.* proposed  $ET_0$  determination using the limited environmental condi-

tions, with help of Temporal Convolution Neural Network (TCN), Long Sort Term Memory Neural Network (LSTM), and Deep Neural Network Model (DNN). The study assesses the performance of these models by different combinations of meteorological conditions. The study compares the proposed model against the Hargreaves (H), Modified Hargreaves (MH), Ritchie (R), Priestley-Talor (PT), and Makkink methods. The study finds that temperature and humidity models to assess the  $ET_0$  rate are better with high  $R^2$  (0.048) and low RMSE (0.096) [17].

Yazid Tikhamarine *et al.* proposed a monthly  $ET_0$  rate estimation using ANN with whale optimization algorithm (ANN-WOA), grey wolf optimizer (ANN-GWO), particle swarm optimizer (ANN-PSO), multi-verse optimizer (ANN-MVO), and ant lion optimizer (ANN-ALO) in Algeria and India [18]. Yazid Tikhamarine *et al.* proposed  $ET_0$  estimation using hybrid Support Vector Regression (SVR) with Whale Optimizer (SVR-WO) with temperature, solar radiation, wind speed, and humidity [5]. Behrooz Keshtegar *et al.* proposed daily  $ET_0$  using subset adaptive neuro-fuzzy inference system (subset ANFIS) [19]. Mohammad Zounemat-Kermani *et al.* proposed a statistical method of Pan-Evaporation (PE) as a soft computational model for two weather stations located in Turkey [20]. Behrooz Keshtegar *et al.* proposed an intelligent approach (SVR-RSM) for the calculation of Pan Evaporation (PE) by combining Support Vector Regression (SVR) and Response Surface Method (RSM) [21]. Ahmed Elbeltagi *et al.* proposed green and blue water  $ET_0$  rates in ArcGIS regions by using geographic information for efficient water management [6]. Yazid Tikhamarine *et al.* proposed a model for improvement in accuracy estimation. The model is based on temperature, humidity, solar radiation, and wind speed. Behrooz Keshtegar and Ozgur Kisi modify the response surface method (RSM) into a hybrid response surface method (HRSM) using the exponential approximation and second-order polynomial estimation. The normalized input dataset is based on the temperature, solar radiation, humidity, and wind speed with application in turkey [22]. Saggi M. and Jain S. proposed the H20 named approach for  $ET_0$  estimation in India. The proposed solution evaluated the performance of the deep learning model of daily  $ET_0$  estimation. The study shows RMSE from 0.1921 to 0.2691 in  $ET_0$  determination using a deep learning approach [23]. Tikhamarine Y. *et al.* proposed hybrid ANN-based  $ET_0$  estimations for India and Algeria. Different ANN hybrid models were compared. ANN-Embedded Grey Wolf Optimizer (ANN-GWO) performs better with RMSE of 0.0592 [18]. Patil A. and Deka P. recommend a solution for weekly  $ET_0$  determination by different combinations of environmental conditions. The proposed solution is implemented in India and the solution is compared against the Hargreaves (H) model. The RMSE of the proposed solution is 0.43 for Jodhpur and 0.33 for Patiala [24]. Adnan M. *et al.* proposed  $ET_0$  estimation with more authenticated and accurate limited meteorological conditions using Deep Learning Neural Network (DNN) model. The regressive value of the proposed

solution is 83% [25]. Ali Rashid Niaghi *et al.* proposed  $ET_0$  estimation from temporal and spatial data using Genome Expression Programming (GEP), Support Vector Machine (SVM), and Linear Regression (LR) models. The performance of the four ML models is evaluated for spatial and temporal data, with GEP performing best on spatial and temporal data [26]. Behrooz Keshtegar *et al.* explored the feasibility of the application of polynomial chaos expansion (PCE) and response surface method (RSM) for modeling  $ET_0$  [10]. The performance of the PCE is evaluated against the M5 model tree and multi-layer perceptron neural network (MLPNN). Shufen Pan *et al.* proposed an ML approach with remote sensing to assess the temporal and spatial  $ET_0$  rate. The findings of the study reveal that there is a 0.62 mm increase in  $ET_0$  rate after every two years [12]. Wang Jing *et al.* evaluated  $ET_0$  approaches by evolutionary approaches and explored the prospects of evolutionary computing approaches in  $ET_0$  determination [13]. Yu Feng *et al.* proposed  $ET_0$  determination using Extreme Machine Learning (EML) approaches and Generalized Neural networks (GNN). The proposed solution is implemented in China. The proposed solution is evaluated against the temperature-based Hargreaves (H) and FAO Penman-Monteith method [27]. Fernandez Lopez *et al.* proposed  $ET_0$  estimation from soil moisture using a regression model and  $K^*$  algorithm. The proposed solution is evaluated against the Penman-Monteith method. The proposed solution shows high accuracy with 0.183 RMSE [28]. Granata F. evaluated the  $ET_0$  estimation models of the MSP regression tree, Bagging Random Forests (BRF), and Support Vector Machine (SVM) with different combinations of meteorological conditions [29]. Pan *et al.* [12] reviewed the variations in global/territorial approaches of  $ET_0$  -rate determination by remote sensing approaches. Krishnan *et al.* [30] recommended Neuro-Fuzzy and Global System for Mobile Communication (GSM) to assist smart irrigation water controllers by incorporating the temperature and humidity. Aggarwal and Kumar [31] recommended soil temperature, moisture, and PH-based irrigation water recommendation. Petković *et al.* [32] recommended a Neuro-Fuzzy approach to determine  $ET_0$  -rate. They suggested that temperature and solar radiations are the most influencing factor of  $ET_0$  -rate determination. Koduru *et al.* [33] proposed IoT and cloud framework for intelligent irrigation systems intending to conserve irrigation water. Yu *et al.* [34] automated the  $ET_0$  -rate determination and suggested a machine, learning-based  $ET_0$  -rate determination model. Angelopoulos *et al.* [35] proposed a smart irrigation system for the strawberry crop to conserve the irrigation water with better yield.

Campos *et al.* [36] proposed smart irrigation water services from monitoring to control of the irrigation water system. The proposed solution recommends the irrigation water according to the soil moisture level. Nawandar *et al.* [37] proposed an intelligent IoT-based smart irrigation system to conserve irrigation water. Fraga-Lamas *et al.* [38] proposed IoT-assisted smart irrigation by exploiting the LoRaWAN-based architecture to avoid the unavailability of

the Internet in remote areas. Leh *et al.* proposed [39] a soil moisture-based smart irrigation water system by assessment of soil moisture conditions for long-distance communication with reduced power consumption. Shi *et al.* [40] suggested a method to determine the Plant Water Deficit Index (PWDI) based on soil moisture conditions and recommend irrigation water accordingly.

Singh *et al.* [41] proposed IoT and ML-based soil moisture assessment to recommend irrigation water accordingly. They assessed the soil moisture based on air temperature, humidity, and radiations from the crop field environmental conditions. Togneri *et al.* [42] recommended IoT and ML-based smart irrigation system that performs a cost-effective customizable analysis. Thakur *et al.* [43] recommended smart irrigation water and integrated it with cloud to convey information regarding irrigation water requirements to end-users. Corbari *et al.* proposed irrigation water requirements estimations based on weather forecasts and satellite-driven water balance models. Michael *et al.* recommended Wireless Sensor Network and Actuator (WSAN) based environmental monitoring and irrigation water control to conserve irrigation water resources [44].

Ajanta Dasgupta *et al.* proposed temperature, humidity, and soil moisture monitoring for irrigation water recommendation according to the prevailing conditions [45]. S Akshay and T K Ramesh proposed an ML-based approach to determine the irrigation water requirements according to the prevailing environmental conditions [46]. Renkuan Liao *et al.* recommend the water uptake depth (WUD) estimation using spatiotemporal characteristics of soil moisture distribution for tomato (*Lycopersicon esculentum*) grown in the greenhouse [47]. Kakkannallur Ethirajan *et al.* recommended IoT-based smart irrigation water systems for hydroponic systems by closely monitoring the water and nutrients flow to improve productivity in these systems [48]. Wang Jing *et al.*, proposed Evolutionary Computing (EC) as the model for the determination of  $ET_0$  with assessment and evaluation [13].

After a comprehensive literature review, it is found that many smart irrigation water application solutions were proposed in recent years with the purpose to conserve irrigation water. Many Wireless Sensor Networks (WSN), and IoT-based crop field monitoring with a purpose to recommend irrigation water according to the environmental conditions. It is observed that smart irrigation water solutions lack in their approach to recommend irrigation water according to the  $ET_0$  rate. On the other hand, many ML approaches were also proposed to determine the  $ET_0$  from limited meteorological conditions. These  $ET_0$  rate determination approaches are not based on real-time crop field meteorological conditions. To accurately determine the crop field  $ET_0$  rate, it must be calculated from directly sensed crop field environmental conditions. To address the deficiencies of both approaches, the study aims to propose  $ET_0$  rate determination with crop field directly sensed temperature and humidity. The proposed solution determines the  $ET_0$  rate by FAO recommended Penman-Monteith  $ET_0$  rate determination method.

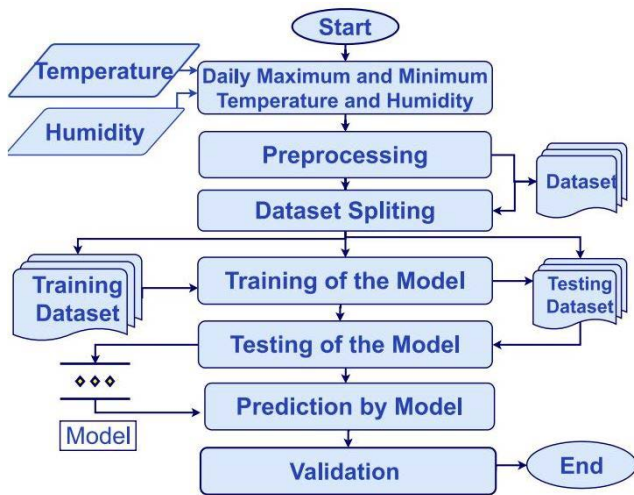


FIGURE 2. Flow chart of proposed solution.

The proposed solution is unique in terms of the use of crop field directly sensed environmental conditions using IoT and following the Penman-Monteith ET<sub>0</sub> method in ET<sub>0</sub> determination using temperature and humidity only.

III. MATERIEL AND METHOD

This section describes the flow chart, the IoT architecture, the prototype, the site of implementation, the sensors used, the environmental data, and the machine learning model.

A. FLOW CHART OF PROPOSED SOLUTION

The flow chart of the proposed solution is shown in Fig. 2. Directly sensed environmental conditions are processed to determine the mean monthly environment conditions. The proposed solution determines the ET<sub>0</sub> rate from temperature and humidity. This daily maximum and minim temperature and humidity are processed to determine the mean temperature and mean humidity. The mean environmental conditions are used to develop the ML model and predict the ET<sub>0</sub> rate by the model. The performance of the model is determined by the test data set. The ET<sub>0</sub> rate is predicted by the ML model and validated by comparing it against the Penman-Monteith method.

B. THE ARCHITECTURE OF INTERNET OF THINGS (IoT) DEVICES

The architecture of IoT devices to sense the crop field environmental conditions is shown in Fig. 3. The crop field temperature, humidity, and wind speed are sensed from the year 2016 to 2021 with the implementation of the IoT architecture. It is a simple architecture with seamless integration of sensor nodes. The data from each sensor node is transferred to the server with help of intermediated gateway nodes and the Internet. The directly sensed crop field environmental conditions by the implementation of the proposed architecture are used to determine the ET<sub>0</sub> by the proposed solution and by the

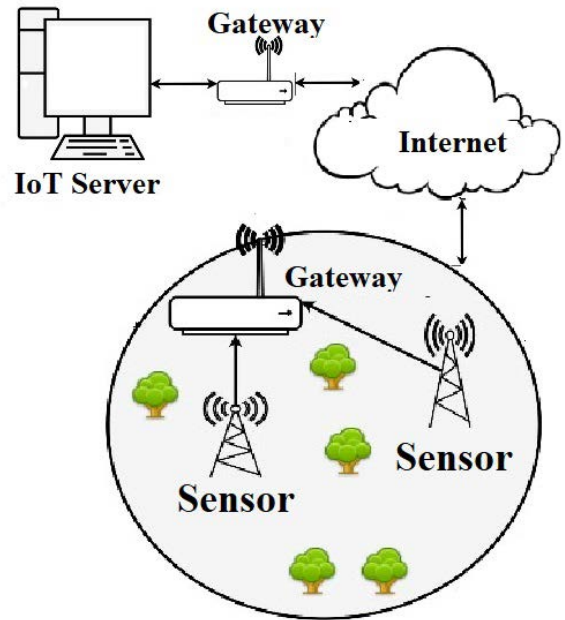


FIGURE 3. Architecture of IoT devices.

Penman-Monteith method. The proposed architecture allows to sense environmental conditions from different fields and recommends ET<sub>0</sub> rate according to these directly sensed crop field environmental conditions. Notably, the communication mode between the gateway and DHT-2 sensor is duplex to facilitate two-way communication.

C. SITE OF IMPLEMENTATION

The proposed solution is implemented in the Multan region of Pakistan which is situated in South East Asia. Pakistan is an agriculture intensive area with arid environmental conditions. The geographical location of the experiment is shown in Fig. 4. The site of implementation is situated at a latitude of 30.1575° N, 71.5249° E, at an altitude of 122 m from sea level. The main reason for this site selection is to evaluate the proposed solutions under a different set of environmental conditions. The variations in weather in Pakistan are very distinct and are suitable to evaluate the proposed solution under different sets of environmental conditions. Pakistan is an agricultural country where 70% of people are linked in agriculture. Pakistan is suffering from irrigation water scarcity. The major reason for irrigation water is poor agronomic practices by the farmers. The application of the proposed solution for irrigation water according to the prevailing ET<sub>0</sub> has many socio-economic implications.

D. SENSORS USED IN THE PROTOTYPE

DHT-2 sensor is used in the prototype to sense the temperature and humidity of the crop field. DHT-2 is a low-cost, low-powered, lightweight, high precision, capacitive type sensor. This is a calibrated digital sensor with long-term stability



FIGURE 4. The geographic location of the experiment area.



FIGURE 5. Temperature and humidity sensor.

TABLE 1. Characteristics of DHT-2 Sensor.

Characteristics	Value
Interface	Serial
Measuring Range	Temperature = -4-80 °C Humidity= 0-100 %
Accuracy	Temperature= +/-1 °C Humidity= +/-0.5 %

without any extra components to measure the surrounding environment. DHT-2 temperature and humidity sensor is shown in Fig. 5, with characteristics in Table 1. In order, to implement the proposed solution the NodeMCU node is used to transfer data from the sensor node to the server with help of the Internet. The NodeMCU is a low-cost, Wi-Fi-enabled module. It is used to transmit data from the sensors to the IoT server using the Internet. It provides an excellent solution to transfer data from the field to the base station using the Internet. The use of NodeMCU makes the architecture portable to move data easily from one area to another. NodeMCU is shown in Fig 6, with characteristics in Table 2.

The prototype developed with IoT architecture to sense the crop field environmental condition is deployed in field is shown in 7.

**E. PENMAN-MONTEITH METHOD**

Penman-Monteith is FAO’s recommended method of ET<sub>0</sub> rate determination. Initially, the Penman-Monteith method of ET<sub>0</sub> is used to determine the ET<sub>0</sub> from prevailing conditions

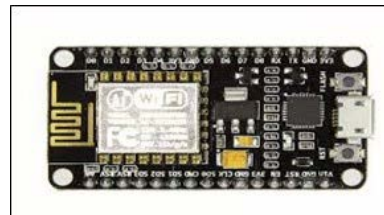


FIGURE 6. NodeMCU gateway module.

TABLE 2. NodeMCU Characteristics.

Characteristics	Value
Interface	Serial
Memory	128 KB
CPU	ESP8266(LX106)
Dimensions	58 mm x 31 mm x 13 mm (LxWxH)



FIGURE 7. Sensor node in crop field.

to train the ML model. It is also used to validate the ET<sub>0</sub> rate proposed by the proposed solution. ET<sub>0</sub> by penman Monteith. Penman-Monteith equation is expressed by Eq. 1 [49]. The ET<sub>0</sub> by the Penman-Monteith method is based on temperature, humidity, wind speed, solar radiations, elevation, and altitude of the location for which ET<sub>0</sub> has to be determined.

$$ET_0 = \frac{(0.408\Delta(R_n - G)) + \gamma \frac{900}{T+273} u_2 (e_s - e_a)}{\Delta + \gamma(1 + 0.34u_2)} \quad (1)$$

where,

- ET<sub>0</sub> is the reference Evapotranspiration in mm day<sup>-1</sup>
- γ is psychrometric constant in KPa°C<sup>-1</sup> expressed by Eq. 2
- Δ is Slope Vapour Pressure in KPa°C<sup>-1</sup> expressed by Eq. 4
- u<sub>2</sub> is wind speed in m s<sup>-1</sup>
- e<sub>s</sub> is saturated vapor pressure in KPa expressed by Eq. 6
- e<sub>a</sub> is actual vapour pressure in KPa expressed by Eq. 7

$e_s - e_a$  is vapour pressure deficit in KPa expressed by Eq. 8

$G$  (soil heat flux density) is the energy used for heating the soil and measured in MJ m<sup>-2</sup> day<sup>-1</sup>. It is very low as compared to  $R_n$  and is ignored for calculating the ET<sub>0</sub>

$R_n$  is the net radiation in crop field measured in MJ m<sup>-2</sup> day<sup>-1</sup> expressed by Eq. 9

$\gamma$  is psychometric constant in KPa<sup>o</sup>C<sup>-1</sup> expressed by Eq. 2

$$\gamma = \frac{C_p P}{\epsilon \lambda} \quad (2)$$

where,  $P$  is the atmospheric pressure in KPa, is the pressure by evaporation at high altitude and the average value of  $P$  is used due to its small effect. The latent heat of vaporization ( $\lambda$ ) is the energy required to change the unit mass of water from liquid to vapor state.  $\epsilon$  is the ratio molecular weight of water vapor measured in MJ Kg<sup>-1</sup>. For simplification, the value of  $\epsilon$  is assumed to be 0.622.  $c_p$  is the specific heat at constant pressure and its value is MJ kg<sup>-1</sup> oC<sup>-1</sup>. Mean monthly temperature ( $T_{mean}$ ) is determined from the mean monthly maximum temperature ( $T_{max}$ ) and mean monthly minimum temperature ( $T_{min}$ ) by Eq. 3.

$$T_{mean} = \frac{T_{max} + T_{min}}{2} \quad (3)$$

Slope of vapour pressure curve ( $\Delta$ ) is the relationship between saturated vapour pressure and temperature expressed by Eq. 4.

$$\Delta = \frac{4098 \left[ 0.6108 \exp \left( \frac{17.27 \times T_{mean}}{T_{mean} + 237.3} \right) \right]}{(T_{mean} + 237.3)^2} \quad (4)$$

where,  $T$  is the air temperature in oC, and  $\Delta$  is the slope of the vapor pressure curve at air temperature in kPa oC.

Saturated Vapour pressure ( $e^o$ ) is obtained from air temperature by Eq. 5, where  $T$  is the air temperature in oC.

$$e^o = 0.6108 \exp \times p \left[ \frac{17.27 T_{mean}}{T + 237.3} \right] \quad (5)$$

Mean Saturated Vapour Pressure ( $e_s$ ) is obtained from Mean monthly maximum temperature ( $T_{max}$ ) and mean monthly minimum temperature ( $T_{min}$ ) and with Saturated Vapour pressure ( $e^o$ ) by Eq. 6.

$$e_s = \frac{e^o(T_{max}) + e^o(T_{min})}{2} \quad (6)$$

Actual vapour pressure ( $e_s$ ) is obtained from mean monthly minimum temperature ( $T_{min}$ ) and mean monthly maximum humidity ( $RH_{max}$ ) by Eq. 7.

$$e_a = e^o(T_{min}) \frac{RH_{max}}{100} \quad (7)$$

Vapour pressure Deficit (VPD) is obtained from actual vapour pressure ( $e_s$ ) and mean saturated vapour pressure ( $e_s$ ) by Eq. 8.

$$VPD = e^s - e^a \quad (8)$$

Net radiation ( $R_n$ ) for ET<sub>0</sub> determination is obtained by difference of radiation that falls on earth surface  $R_{ns}$  and radiations that reflected back from earth surface  $R_{nl}$ , expressed by Eq. 9.

$$R_n = R_{ns} - R_{nl} \quad (9)$$

Radiation that falls on earth surface  $R_{ns}$  is the fraction of solar radiation  $R_s$  that is not reflected by the earth surface expressed by Eq. 10. For ET of grass crop, the value of  $\alpha$  is 0.23, therefore the value of  $R(ns)$  is expressed by Eq. 11.

$$R_{ns} = (1 - \alpha) \times R_s \quad (10)$$

$$R_{nl} = 0.77 \times R_s \quad (11)$$

Solar radiation ( $R_s$ ) is obtained by Hargreaves model of solar radiation expressed by Eq. 12, from mean monthly maximum temperature ( $T_{max}$ ), mean monthly minimum temperature ( $T_{min}$ ), extraterritorial radiation ( $R_a$ ), and adjustment constant ( $K_{Rs}$ ).

$$R_s = K_{Rs} \sqrt{T_{max} - T_{min}} R_a \quad (12)$$

Radiation that reflected from earth surface  $R_{nl}$  is obtained by the Stefan-Boltzman law expressed by Eq. 13

$$R_{nl} = \sigma \left[ \frac{T_{max} K^4 + T_{min} K^4}{(1.35 \frac{R_s}{R_{so}} - 0.35)} \right] (0.34 - 0.14 \sqrt{e_a}) \quad (13)$$

where,

$T_{max} K$  is mean monthly maximum temperature in Kelvin scale,

$T_{min} K$  is mean monthly minimum temperature in Kelvin scale,

$\sigma$  is the Stefan Boltzmann constant that is  $5.670367 \times 10^{-8}$  kg s<sup>-3</sup> K<sup>-4</sup>

$e_a$  is the actual vapour pressure,

$\frac{R_s}{R_{so}}$  is the ratio of the solar radiation that reaches to the earth surface in clear sky ( $R_s$ ) to the solar radiations that reaches to the earth surface in cloudy conditions ( $R_{so}$ ). It is the relative shortwave radiation (limited to  $\leq 1.0$ ), where  $R_s$  is obtained by Eq. 12, and is obtained by Eq. 14. Notably,  $Z$  is the elevation above sea level measured in meters.

$$R_{so} = (0.75 + 210^{-5} Z) R_a \quad (14)$$

## F. ENVIRONMENTAL DATA

In this section, the environmental data of temperature, humidity, and wind speed directly sensed from the crop field is given. The data from the year 2016 to 2021 is used to train, test, and validate the model. The temperature data analysis is shown in Fig. 8, Fig. 9, Fig. 10, Fig. 11, Fig. 12, and Fig. 13 for the year 2016 to 2021 respectively. The daily maximum temperature, daily minimum temperature and mean monthly temperature are shown in each figure.

Humidity is also important for the determination of ET<sub>0</sub> by the proposed solution and by the Penman-Monteith method. Humidity data of the selected area from the year 2016 to

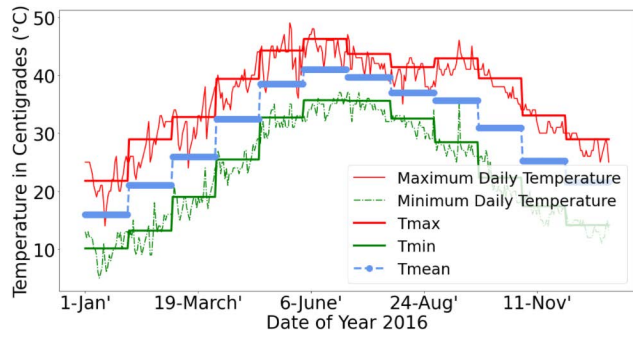


FIGURE 8. Temperature of 2016.

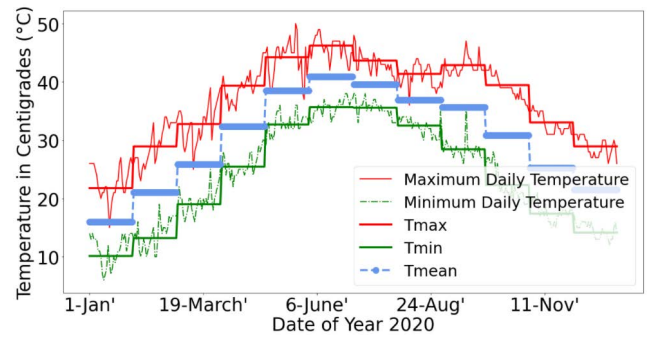


FIGURE 12. Temperature of 2020.

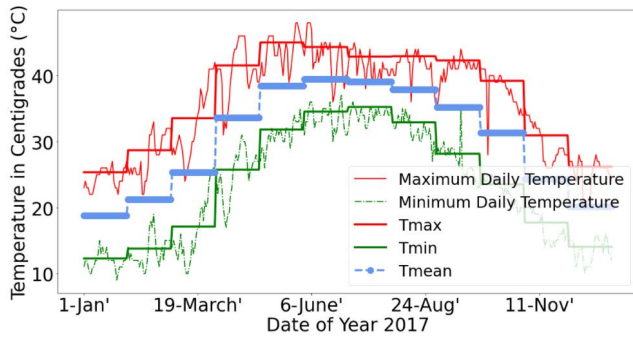


FIGURE 9. Temperature of 2017.

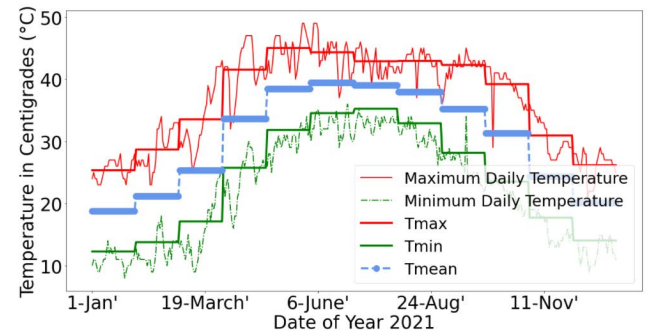


FIGURE 13. Temperature of 2021.

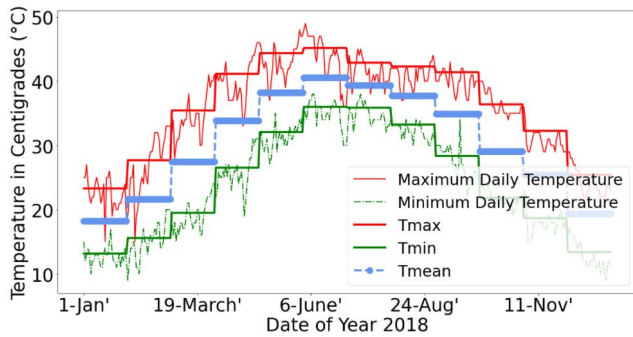


FIGURE 10. Temperature of 2018.

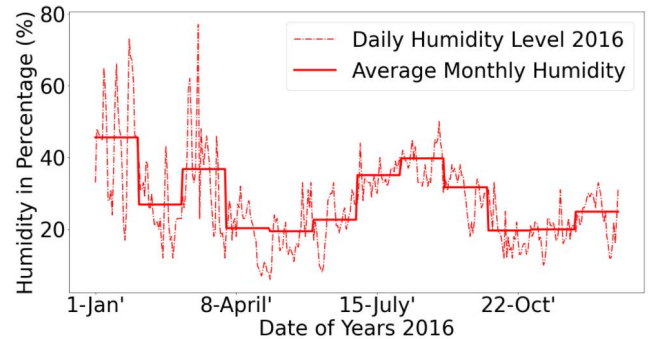


FIGURE 14. Humidity level for the year 2016.

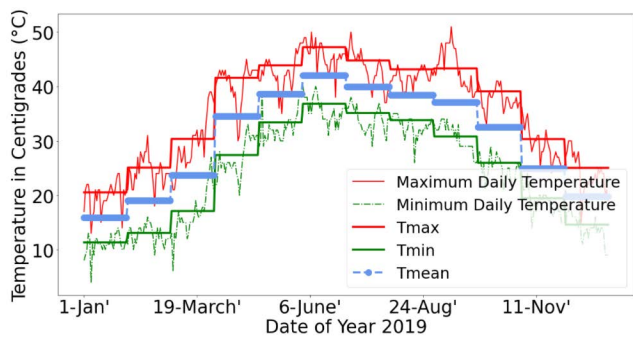


FIGURE 11. Temperature of 2019.

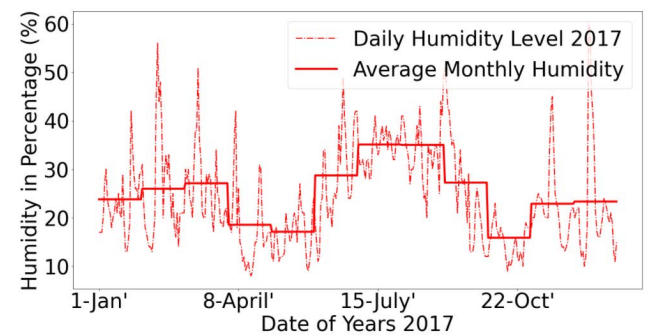


FIGURE 15. Humidity level for the year 2017.

2021 is sensed from the crop field using an IoT prototype. Along with daily maximum humidity levels, the mean monthly humidity level ( $H_m$ ) is also plotted in each fig-

ure. Fig. 14, Fig. 15, Fig.16, Fig.17, Fig.18, and Fig.19 shows daily maximum and mean monthly humidity from year 2016 to 2021. respectively.



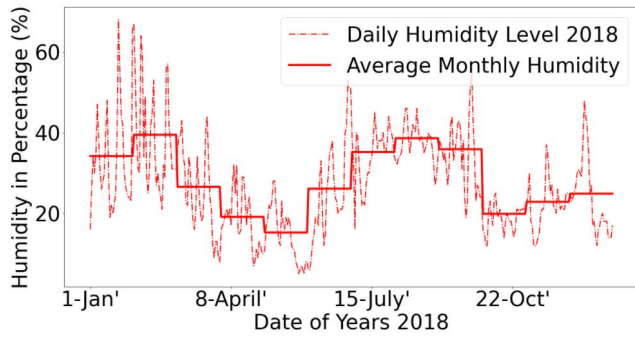


FIGURE 16. Humidity level for the year 2018.

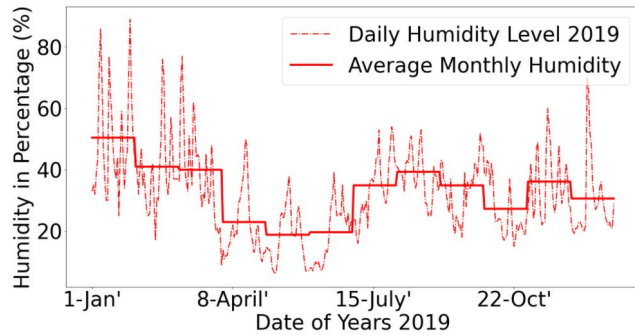


FIGURE 17. Humidity level for the year 2019.

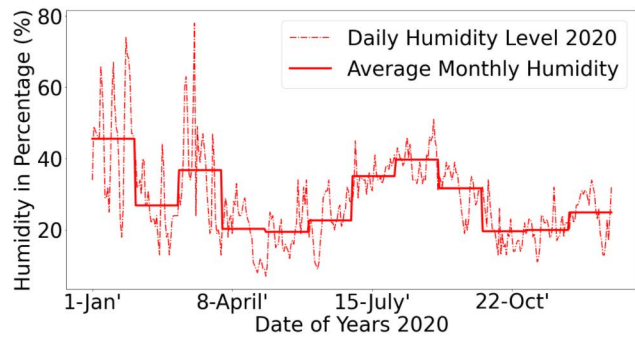


FIGURE 18. Humidity level for the year 2020.

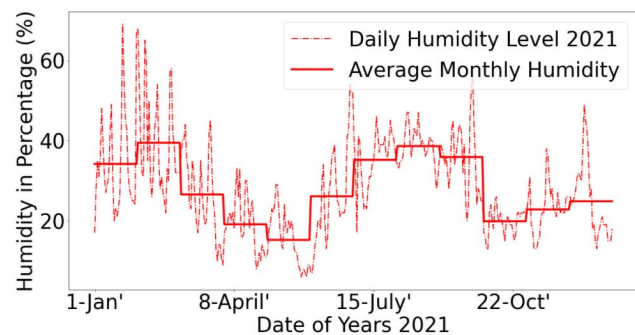


FIGURE 19. Humidity level for the year 2021.

Win speed is also important for the determination of  $ET_0$  by the Penman-Monteith method. Wind speed data of the selected area from the year 2016 to 2021 is sensed from the

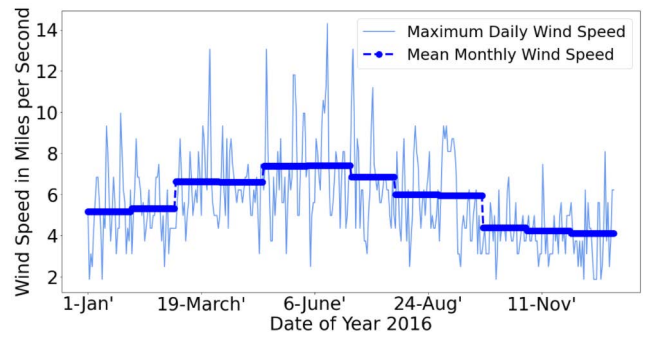


FIGURE 20. Wind speed for the year 2016.

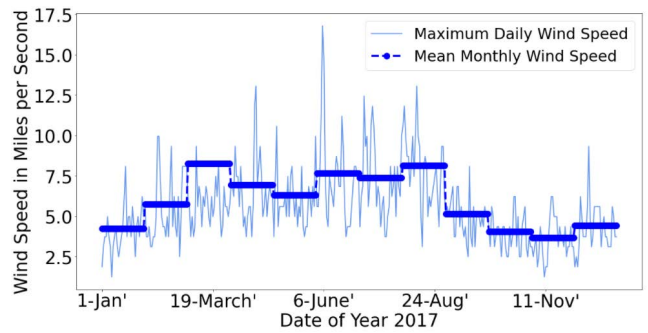


FIGURE 21. Wind speed for the year 2017.

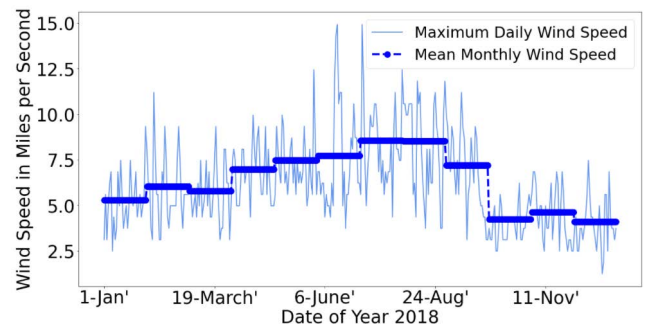


FIGURE 22. Wind speed for the year 2018.

crop field using an IoT prototype. Along with daily maximum wind speed, the mean monthly wind speed is also plotted in each figure. Fig. 20, Fig. 21, Fig.22, Fig.23, Fig.24, and Fig.25 shows daily maximum and mean monthly wind speed from year 2016 to 2021 respectively.

### G. MACHINE LEARNING MODEL

For ML model implementation the Support Vector Machine (SVM), K-Nearest Neighbour (KNN), and Gaussian Naive Bays (GNB) based models are implemented. The tuple of environmental conditions is used to classify the  $ET_0$  rate in “low”, “medium” and “high” as per the  $ET_0$  classification given in the Table 5. The data set is partitioned into predictive features and response vectors. Each predictive feature vector is based on temperature and humidity to predict

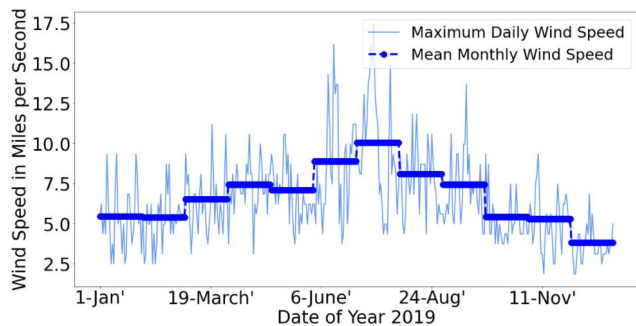


FIGURE 23. Wind speed for the year 2019.

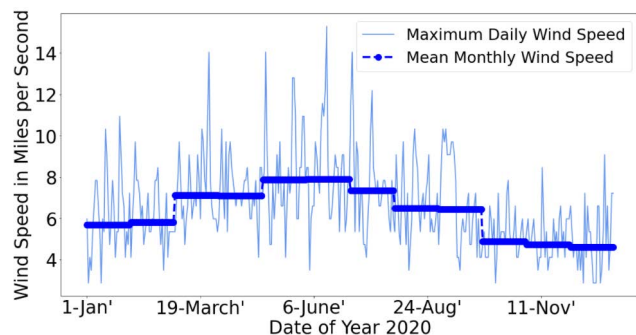


FIGURE 24. Wind speed for the year 2020.

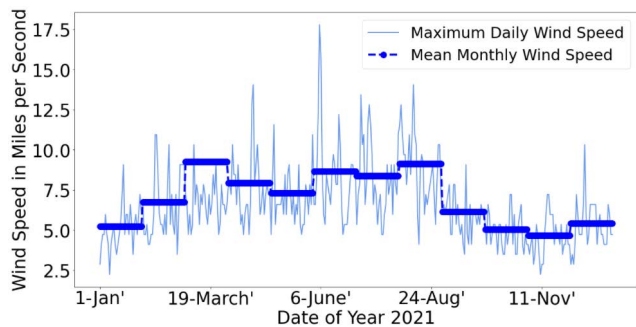


FIGURE 25. Wind speed for the year 2021.

the ET<sub>0</sub> response vector. The predictive features vector is also arranged according to the suitable class range given in Table 3, and Table 4. To implement the machine learning algorithms, the Scikit-learn libraries of python are used to preprocess, train and test the ML model. Classes for temperature, humidity, and ET<sub>0</sub> rate are given in Table 3, Table 4, and Table 5, respectively. The data from the year 2016 to 2021 is used to train the ML model. The study use the daily climatic conditions from year 2016 to 2021. Yellowbrick library is used for testing the ML model. The first step in data preprocessing is data organization. The directly sensed crop field temperature and humidity is used to determine the daily maximum and minimum temperature and humidity. The daily minimum and maximum temperature and humidity are used to predict the *Et<sub>o</sub>* rate. After data organization, the missing

TABLE 3. Temperature classes.

Temperature Range (°C)	Class
<25	Low
25-40	Medium
>40	High

TABLE 4. Humidity classes.

Humidity Range (%)	Class
<30	Low
30-70	Medium
>70	High

TABLE 5. ET<sub>0</sub> rate classes.

ET <sub>0</sub> Range in mm/day	Class
<5	Low
5-8	Medium
>8	High

values are identified and handled for data cleaning purposes. The data cleaning is handled by filling the missing values through the mean value of corresponding months from the previous year. This approximation of missing data by mean produces minimum bias. The next step is the encoding of the categorical items in the data like months name. After data partitioning, the dataset is split into training and test dataset. The ratio of training to test data set is set to 70:30. To avoid extreme values, the feature scaling is performed by standardization using the preprocessing featured of sklearn libraries of python. The standardization is performed by Eq. 15 where missing value 'a' in dataset is approximated by *a'*.

$$\hat{a} = \frac{a - (mean)}{sd} \tag{15}$$

The study also apply the Artificial Neural Network Model (ANN) to assess the performance of the ML models. The proposed ANN architecture aims to determine the ET<sub>0</sub> rate from independent variables Tmax, Tmin, Hmax, and Hmin. Multilayered perception feed forward neural network architecture is used for implementation of ANN for ET<sub>0</sub> rate determination. The number of neurons are equal to the number of input variables and one neuron at the output layer. The neuron in each layer is connected to subsequent layer by weights *w<sub>i</sub>* and from hidden layer to output layer by weight. Each neuron the sum of input variables with their weights is transformed into output with activation function. Relu activation function is used at input and hidden layer and sigmoid at output layer. The inputs are propagated from input to hidden layer and from hidden layer to the output layer in forward manner. In order to prevent convergence

TABLE 6. Accuracy of machine learning models.

Machine Learning Model	Accuracy (%)
Linear SVM	88
K-Nearest Neighbour	92
Guassian Naive Bays	85
ANN	91

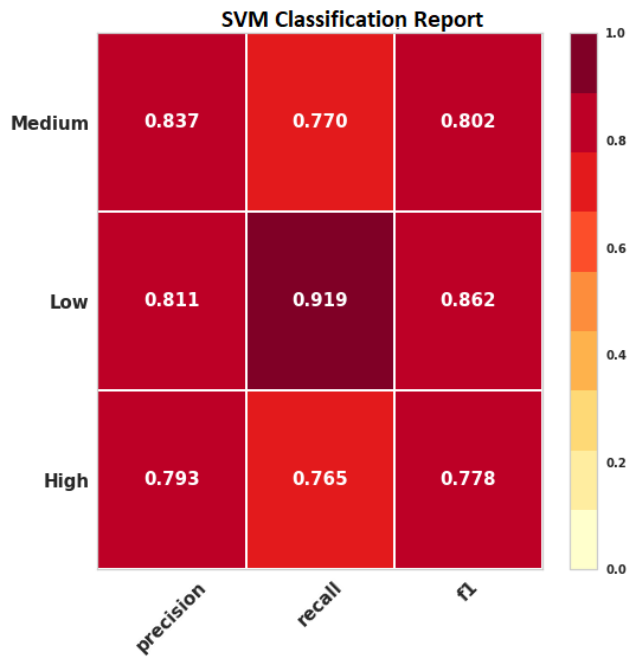


FIGURE 26. Confusion matrix of SVM model.

issue all the inputs are normalized before passing them to ANN architecture. The dataset of the input variables is used as input and corresponding ET<sub>0</sub> is the output of the model. The input and output variables are standardized before passing to ANN mode. The number of neurons at hidden layer are identified by hit and trial method with a purpose to improve the performance of the model. The best ANN architecture of ANN for the study is 4-3-1 that means four neurons at input layer, three at hidden layer and one at the output layer.

IV. RESULTS

The results are given in the form of accuracy of SVM, KNN and GNB ML models and confusion matrix of each model. The Root Mean Squared Errors (RMSE) and Mean Absolute Error (MAE) are used to compare the performance with existing solution. The ET<sub>0</sub> by proposed solution is also compared against the Penman-Montieth method for validation of the proposed solution.

A. PERFORMANCE OF ML ALGORITHMS

The training and test data ratio is set to (70:30) for evaluation purposes. Performance of the machine learning algorithms

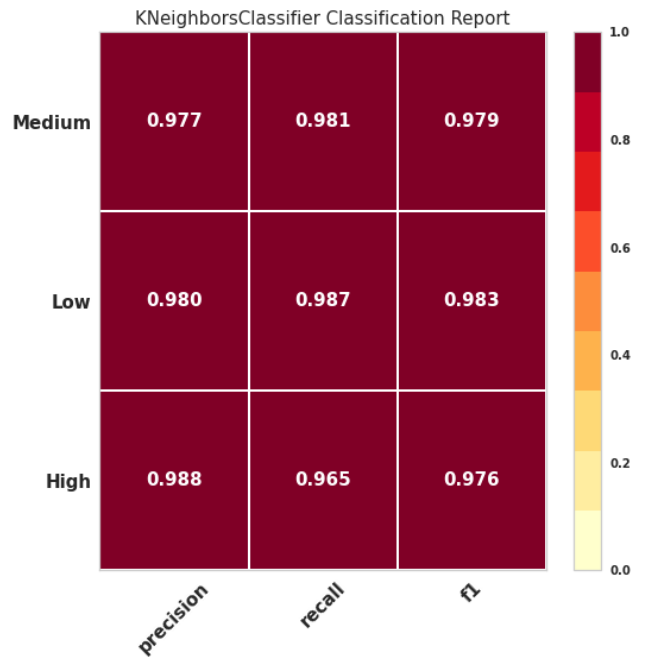


FIGURE 27. Confusion matrix of KNN model.

is determined using the accuracy of the different algorithms with test data is given in Table 6. Accuracy of the KNN model in ET<sub>0</sub> determination is 91% that is more than the GNB, SVM and ANN. The confusion matrices of SVM, KNN, GNB and ANN is shown in Fig. 26, Fig. 27, Fig. 28 and in 28 respectively. The precision, recall and f-measure of KNN is better as compared to the SVM and GNB in prediction of ET<sub>0</sub> from temperature and humidity. In case of ML models the accuracy of ET<sub>0</sub> prediction is better with KNN model than the SVM and GNB model. Apart from the accuracy the KNN models also has some inherent advantages that are favourable to apply it for problem on hand. The advantage of the application of KNN is that new data can be added seamless manner without much impact on accuracy of existing model. This is very important in case of a problem on hand. New data from each year can be easily added to improve the accuracy of predictions made by the model. The sensed data from the crop field can be added in a seamless manner. The other advantage of KNN is that it is easy to implement as compared to other ML models. The KNN also shows good accuracy with limited dataset as in the case of problem on hand.

B. COMPARISON WITH EXISTING APPROACHES

The result of the proposed solution are compared against the Al Rashid Niaghi proposed method of ET<sub>0</sub> estimation using three ML algorithm named Random Forest (RF), Support Vector Machine (SVM) and Multiple Linear Regression (M-LR) with local and spatial environmental conditions [26]. The study evaluated the performance of the different machine learning algorithms in terms of Root Mean Squared Error (RMSE) and Mean Absolute Error (MAE)

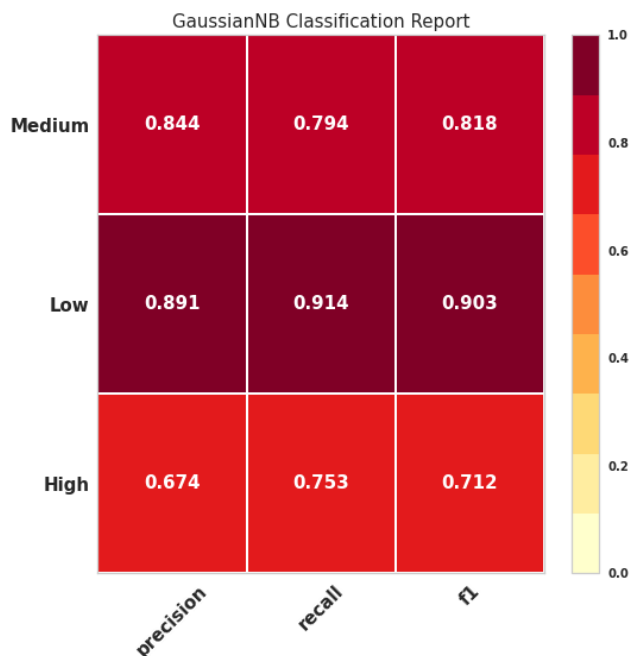


FIGURE 28. Confusion matrix of GNB model.

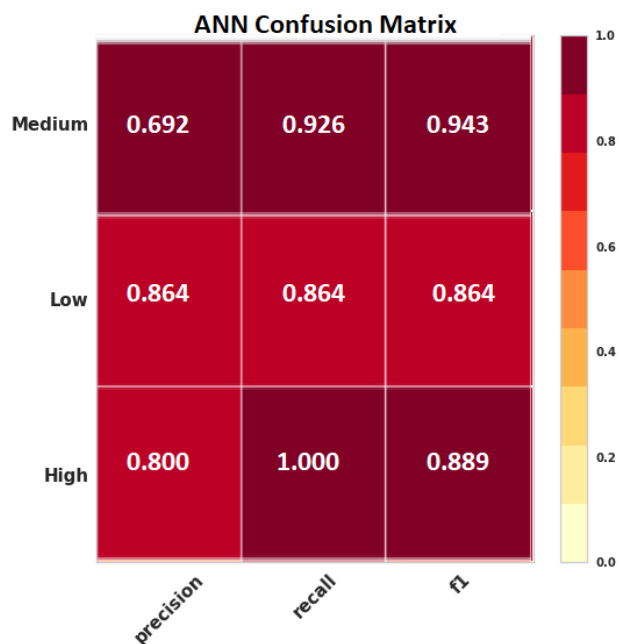


FIGURE 29. Confusion matrix of ANN model.

with different combination of input conditions. The ML algorithms are evaluated using temporal, radiations and mass transfer based method. The results of the temporal and radiation based method by [26] and by our proposed solution is given in Table 7. The solution proposed by [26] find out that in case of temporal method the RMSE by GEP model reduces by 7% as compared to the SVM and LR models. GEP also reduce Mean Absolute Errors (MAE) by 7% as compared to

TABLE 7. Comparison with existing approaches.

Approach Description	ML Model	RMSE (mm day <sup>-1</sup> )	MAE (mm day <sup>-1</sup> )
Existing Temporal [26]	SVM	0.97	0.71
Existing Temporal [26]	LR	0.97	0.76
Existing Temporal [26]	GEP	0.90	0.64
Existing Radiation [26]	SVM	0.72	0.54
Existing Radiation [26]	LR	0.68	9.51
Existing Radiation [26]	GEP	0.71	0.50
Proposed	KNN	0.74	0.61
Proposed	SVM	0.88	0.90
Proposed	GNB	0.91	0.89
Proposed	ANN	0.75	0.62

SVM and 12% as compared to LR in case of tempera data. In case of radiation approach LR reduces the RMSE 4% more than the SVM, and 6% more then the GEP. Whereas in case of radiation based approach the GEP reduces MAE by 1% from the LR and 4% from the SVM. In case [26] of GEP reduces RMSE and MAE by temporal and radiation based approach for ET<sub>0</sub> estimation. In case of proposed solution the KNN model reduces the RMSE by 14% more than the SVM and 17% more than the GNB model. The KNN model outperform the SVM and GNB in reduction of the RMSE. The KNN mode reduces the MAE by 29% more than the SVM and 28% more than the GNB model. As compared to existing approach [26], the KNN reduce the RMSE errors against the GEP models by 16% and MAE by 3%.

C. FIELD OBSERVATIONS

The ET<sub>0</sub> rate determined from the proposed solution is compared against the FAO-recommended Penman-Monteith method of ET<sub>0</sub> determination. The ET<sub>0</sub> rate from the proposed solution is named as predicted (ET<sub>0</sub>) and by the Penman-Monteith method as actual ET<sub>0</sub>. The comparison of predicted (ET<sub>0</sub>) and actual ET<sub>0</sub> rate is compared on monthly basis for each year from 2016 to 2021. The ET<sub>0</sub> rate for the year 2016, by proposed solution and by Penman-Monteith method is shown in Fig. 30. There is a very low difference in predicted and actual ET<sub>0</sub> rate by proposed solution and by the Penman-Monteith method for each month of the year 2016. The maximum difference is observed in March, April and May that is 1.8 mm day<sup>1</sup>. The minimum difference of ET<sub>0</sub> rate is observed in October that is of 0.2 mm day<sup>1</sup>. The difference in ET<sub>0</sub> observation for the year 2016, can be observed from Fig. 36. The ET<sub>0</sub> rate for the year 2017, by proposed solution and by Penman-Monteith method is shown in Fig. 31. There is also low difference in predicted and actual ET<sub>0</sub> rate by proposed solution and by the Penman-Monteith method for each month of the year 2017. The maximum difference is observed in March that is 2 mm day<sup>1</sup>. The

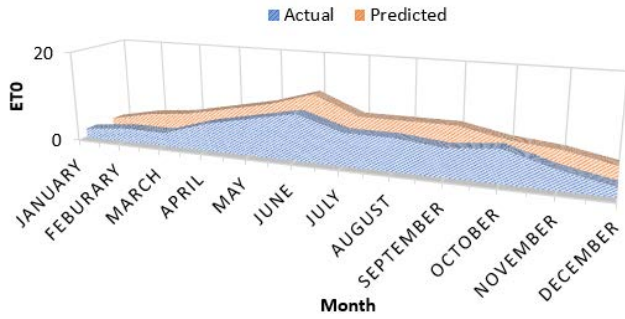


FIGURE 30. Actual and predicted ET<sub>0</sub> rate of 2016.

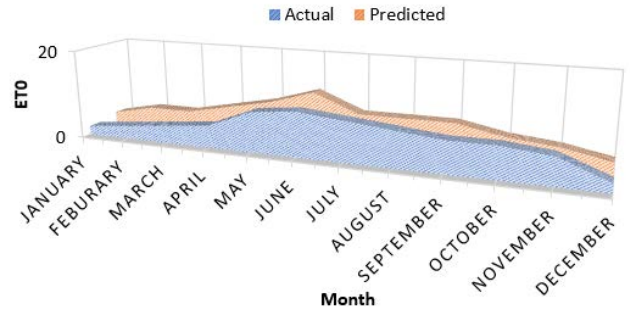


FIGURE 33. Actual and predicted ET<sub>0</sub> rate of 2019.

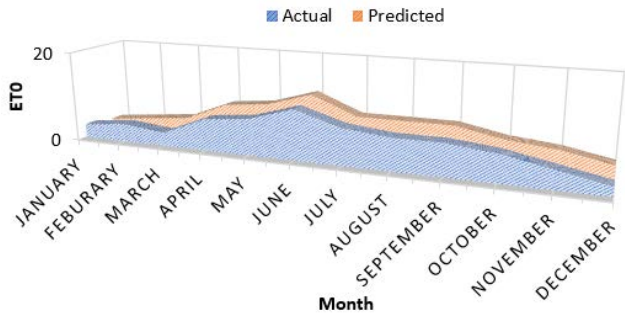


FIGURE 31. Actual and predicted ET<sub>0</sub> rate of 2017.

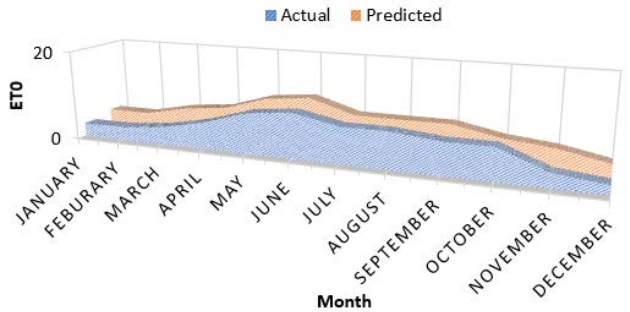


FIGURE 34. Actual and predicted ET<sub>0</sub> rate of 2020.

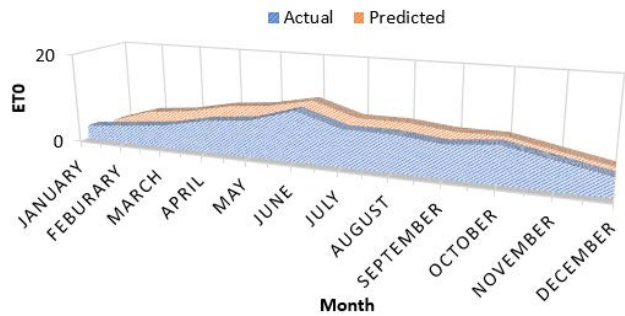


FIGURE 32. Actual and predicted ET<sub>0</sub> rate of 2018.

minimum difference of ET<sub>0</sub> rate is observed in January that is of 0.5 mm day<sup>-1</sup>. The difference in ET<sub>0</sub> observation for the year 2017, can be observed from Fig. 36. The ET<sub>0</sub> rate for the year 2018, by proposed solution and by Penman-Monteith method is shown in Fig. 32. There is also low difference in predicted and actual ET<sub>0</sub> rate by proposed solution and by the Penman-Monteith method for each month of the year 2018. The maximum difference is observed in February and May that is 1.4 mm day<sup>-1</sup>. The minimum difference of ET<sub>0</sub> rate is observed in September that is of 0.1 mm day<sup>-1</sup>. The difference in ET<sub>0</sub> observation for the year 2018, can be observed from Fig. 36. The ET<sub>0</sub> rate for the year 2019, by proposed solution and by Penman-Monteith method is shown in Fig. 33. There is also low difference in predicted and actual ET<sub>0</sub> rate by proposed solution and by the Penman-Monteith method for

each month of the year 2019. The maximum difference is observed in February and June that is 1.9 mm day<sup>-1</sup>. The minimum difference of ET<sub>0</sub> rate is observed in May and July that is of 0.3 mm day<sup>-1</sup>. The difference in ET<sub>0</sub> observation for the year 2019, can be observed from Fig. 36. The ET<sub>0</sub> rate for the year 2020, by proposed solution and by Penman-Monteith method is shown in Fig. 34. There is also low difference in predicted and actual ET<sub>0</sub> rate by proposed solution and by the Penman-Monteith method for each month of the year 2020. The maximum difference is observed in June and November that is 1.9 mm day<sup>-1</sup>. The minimum difference of ET<sub>0</sub> rate is observed in July that is of 0.8 mm day<sup>-1</sup>. The difference in ET<sub>0</sub> observation for the year 2020, can be observed from Fig. 36. The ET<sub>0</sub> rate for the year 2021, by proposed solution and by Penman-Monteith method is shown in Fig. 35. There is also low difference in predicted and actual ET<sub>0</sub> rate by proposed solution and by the Penman-Monteith method for each month of the year 2021. The maximum difference is observed in January that is 2.1 mm day<sup>-1</sup>. The minimum difference of ET<sub>0</sub> rate is observed in January that is of 0.3 mm day<sup>-1</sup>. The difference in ET<sub>0</sub> observation for the year 2021, can be observed from Fig. 36.

The proposed solution is accurate in the determination of the ET<sub>0</sub> rate of a location on the directly observed temperature and humidity of that location. The ET<sub>0</sub> rate by proposed solution shows accuracy when compared against the Agronomist recommended Penman-Monteith method of ET<sub>0</sub> determination.

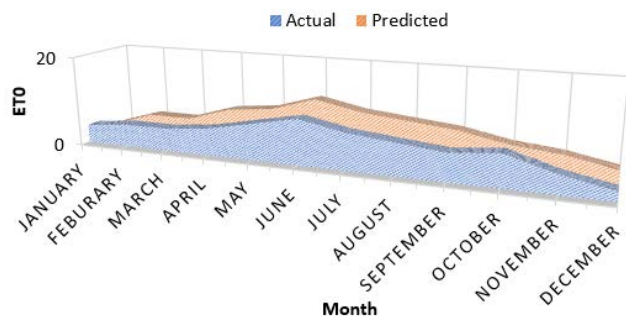


FIGURE 35. Actual and predicted ET rate of 2021.

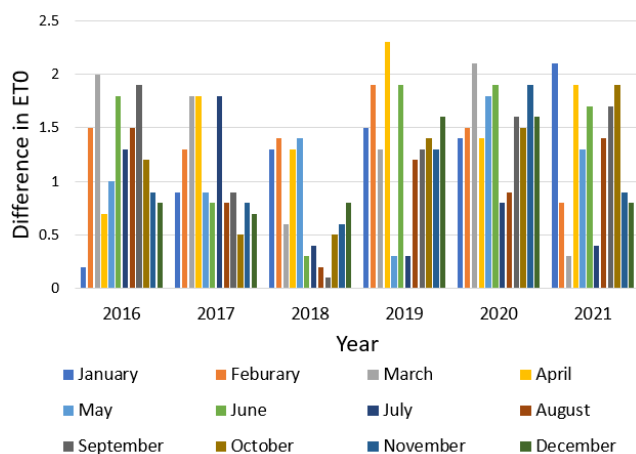


FIGURE 36. Difference in observations by proposed and Penman-Monteith method.

Many solutions were proposed to determine the ET<sub>0</sub> in past. These solutions are limited to one or two geographical areas. There is need of a solution that is applicable at global scale. The major purpose of the proposed solution is to propose a global solution that can be applied to any part of the world by using IoT. The directly sensed environmental conditions help to propose a solution that is easily transferable and applicable in any part of the world. The proposed solutions sense the crop field environmental conditions to predict the ET<sub>0</sub> rate according to the locations where the solution is applied. The proposed solution is easily transferable and applicable in any part of the world to adjust according to the prevailing conditions. The unique feature of the proposed solution is the prediction of the ET<sub>0</sub> rate based on directly sensed environmental conditions that can easily be implemented by the proposed IoT architecture. The direct crop field sensed environmental conditions-based ET<sub>0</sub> solution make the proposed solution application on a global scale rather than confined to any limited geographical areas.

## V. CONCLUSION

The directly sensed crop field temperature and humidity based Evapotranspiration (ET<sub>0</sub>) prediction in accordance with Penman-Monteith method is proposed. Machine Learning (ML) based ET<sub>0</sub> rate determination from IoT assisted

directly sensed temperature and humidity from the crop field is proposed. ET<sub>0</sub> determination with limited environmental condition is important. The proposed solution determines the ET<sub>0</sub> rate according to the Penman-Monteith method. The crop field environment conditions are captured using the IoT-assisted proposed architecture. The proposed solution supports smart irrigation by conservation of irrigation water while maintaining yield. Three machine learning algorithms K-nearest Neighbour (KNN), Gaussian Naive Bays (GNB), Support Vector Machine (SVM) and Artificial Neural Network (ANN) are compared for accuracy in determination of ET<sub>0</sub>. It is observed that KNN is more accurate with 92% accuracy, with high precision, recall and f-measure as compared to the SVM and GNB models. The field observations from 2016 to 2021 are used to validate the proposed solution. The proposed solution of ET<sub>0</sub> determination by temperature and humidity is accurate in the determination of ET<sub>0</sub> rate when compared against the FAO recommended Penman-Monteith method. As concerned of future work the use of federated learning would be a good contribution to handle on problem of global scale application and transfer in better way.

## REFERENCES

- [1] S. Maurya and V. K. Jain, "Fuzzy based energy efficient sensor network protocol for precision agriculture," *Comput. Electron. Agricult.*, vol. 130, pp. 20–37, Nov. 2016.
- [2] *Global Agriculture Towards 2050*, FAO, Rome, Italy, 2009, pp. 1–4.
- [3] T. Qian, A. Tsunekawa, F. Peng, T. Masunaga, T. Wang, and R. Li, "Derivation of salt content in salinized soil from hyperspectral reflectance data: A case study at Minqin Oasis, Northwest China," *J. Arid Land*, vol. 11, no. 1, pp. 111–122, Feb. 2019.
- [4] A. Malik, A. Kumar, M. A. Ghorbani, M. H. Kashani, O. Kisi, and S. Kim, "The viability of co-active fuzzy inference system model for monthly reference evapotranspiration estimation: Case study of Uttarakhand state," *Hydrol. Res.*, vol. 50, no. 6, pp. 1623–1644, Dec. 2019.
- [5] Y. Tikhmarine, A. Malik, K. Pandey, S. S. Sammen, D. Souag-Gamane, S. Heddami, and O. Kisi, "Monthly evapotranspiration estimation using optimal climatic parameters: Efficacy of hybrid support vector regression integrated with whale optimization algorithm," *Environ. Monit. Assessment*, vol. 192, no. 11, pp. 1–19, Nov. 2020. [Online]. Available: <https://link.springer.com/article/10.1007/s10661-020-08659-7>
- [6] A. Elbeltagi, M. R. Aslam, A. Mokhtar, P. Deb, G. A. Abubakar, N. L. Kushwaha, L. P. Venancio, A. Malik, N. Kumar, and J. Deng, "Spatial and temporal variability analysis of green and blue evapotranspiration of wheat in the Egyptian Nile delta from 1997 to 2017," *J. Hydrol.*, vol. 594, Mar. 2021, Art. no. 125662.
- [7] Y. Tikhmarine, A. Malik, D. Souag-Gamane, and O. Kisi, "Artificial intelligence models versus empirical equations for modeling monthly reference evapotranspiration," *Environ. Sci. Pollut. Res.*, vol. 27, no. 24, pp. 30001–30019, Aug. 2020. [Online]. Available: <https://link.springer.com/article/10.1007/s11356-020-08792-3>
- [8] J. M. Talavera, L. E. Tobón, J. A. Gómez, M. A. Culman, J. M. Aranda, D. T. Parra, L. A. Quiroz, A. Hoyos, and L. E. Garreta, "Review of IoT applications in agro-industrial and environmental fields," *Comput. Electron. Agricult.*, vol. 142, no. 1, pp. 283–297, 2017.
- [9] B. Keshtegar, S. S. Abdullah, Y. F. Huang, M. K. Saggi, K. M. Khedher, and Z. M. Yaseen, "Reference evapotranspiration prediction using high-order response surface method," *Theor. Appl. Climatol.*, vol. 148, nos. 1–2, pp. 849–867, Apr. 2022. [Online]. Available: <https://link.springer.com/article/10.1007/s00704-022-03954-4>
- [10] B. Keshtegar, O. Kisi, and M. Zounemat-Kermani, "Polynomial chaos expansion and response surface method for nonlinear modelling of reference evapotranspiration," *Hydrol. Sci. J.*, vol. 64, no. 6, pp. 720–730, Apr. 2019. [Online]. Available: <https://www.tandfonline.com/doi/abs/10.1080/02626667.2019.1601727>, doi: 10.1080/02626667.2019.1601727.

- [11] L. B. Ferreira and F. F. da Cunha, "New approach to estimate daily reference evapotranspiration based on hourly temperature and relative humidity using machine learning and deep learning," *Agricult. Water Manage.*, vol. 234, May 2020, Art. no. 106113.
- [12] S. Pan, N. Pan, H. Tian, P. Friedlingstein, S. Sitch, H. Shi, V. K. Arora, V. Haverd, A. K. Jain, E. Kato, S. Lienert, D. Lombardozi, J. E. M. S. Nabel, C. Otlé, B. Poulter, S. Zaehle, and S. W. Running, "Evaluation of global terrestrial evapotranspiration using state-of-the-art approaches in remote sensing, machine learning and land surface modeling," *Hydrol. Earth Syst. Sci.*, vol. 24, no. 3, pp. 1485–1509, Mar. 2020.
- [13] W. Jing, Z. M. Yaseen, S. Shahid, M. K. Saggi, H. Tao, O. Kisi, S. Q. Salih, N. Al-Ansari, and K.-W. Chau, "Implementation of evolutionary computing models for reference evapotranspiration modeling: Short review, assessment and possible future research directions," *Eng. Appl. Comput. Fluid Mech.*, vol. 13, no. 1, pp. 811–823, Jan. 2019.
- [14] Z. Turgut, G. Z. G. Aydin, and A. Sertbas, "Indoor localization techniques for smart building environment," *Proc. Comput. Sci.*, vol. 83, pp. 1176–1181, Jan. 2016.
- [15] F. Bu and X. Wang, "A smart agriculture IoT system based on deep reinforcement learning," *Future Gener. Comput. Syst.*, vol. 99, pp. 500–507, Oct. 2019.
- [16] S. S. Yamaç and M. Todorovic, "Estimation of daily potato crop evapotranspiration using three different machine learning algorithms and four scenarios of available meteorological data," *Agricult. Water Manage.*, vol. 228, Feb. 2020, Art. no. 105875.
- [17] Z. Chen, Z. Zhu, H. Jiang, and S. Sun, "Estimating daily reference evapotranspiration based on limited meteorological data using deep learning and classical machine learning methods," *J. Hydrol.*, vol. 591, Dec. 2020, Art. no. 125286.
- [18] Y. Tikhmarine, A. Malik, A. Kumar, D. Souag-Gamane, and O. Kisi, "Estimation of monthly reference evapotranspiration using novel hybrid machine learning approaches," *Hydrol. Sci. J.*, vol. 64, no. 15, pp. 1824–1842, Nov. 2019. [Online]. Available: <https://www.tandfonline.com/doi/10.1080/02626667.2019.1678750>.
- [19] B. Keshtegar, O. Kisi, H. G. Arab, and M. Zounemat-Kermani, "Subset modeling basis ANFIS for prediction of the reference evapotranspiration," *Water Resour. Manage.*, vol. 32, no. 3, pp. 1101–1116, Feb. 2018. [Online]. Available: <https://link.springer.com/article/10.1007/s11269-017-1857-5>.
- [20] M. Zounemat-Kermani, B. Keshtegar, O. Kisi, and M. Scholz, "Towards a comprehensive assessment of statistical versus soft computing models in hydrology: Application to monthly pan evaporation prediction," *Water*, vol. 13, no. 17, p. 2451, Sep. 2021.
- [21] B. Keshtegar, S. Heddami, A. Sebban, S.-P. Zhu, and N.-T. Trung, "SVR-RSM: A hybrid heuristic method for modeling monthly pan evaporation," *Environ. Sci. Pollut. Res.*, vol. 26, no. 35, pp. 35807–35826, Dec. 2019. [Online]. Available: <https://pubmed.ncbi.nlm.nih.gov/31705408/>.
- [22] B. Keshtegar and O. Kisi, "Modified response-surface method: New approach for modeling pan evaporation," *J. Hydrol. Eng.*, vol. 22, no. 10, Oct. 2017, Art. no. 04017045.
- [23] M. K. Saggi and S. Jain, "Reference evapotranspiration estimation and modeling of the Punjab northern India using deep learning," *Comput. Electron. Agricult.*, vol. 156, pp. 387–398, Jan. 2019.
- [24] A. P. Patil and P. C. Deka, "An extreme learning machine approach for modeling evapotranspiration using extrinsic inputs," *Comput. Electron. Agricult.*, vol. 121, pp. 385–392, Feb. 2016.
- [25] M. Adnan, M. Ahsan, A. U. Rehman, and M. Nazir, "Estimating evapotranspiration using machine learning techniques," *Int. J. Adv. Comput. Sci. Appl.*, vol. 8, no. 9, pp. 108–113, 2017.
- [26] A. R. Niaghi, O. Hassanijalilian, and J. Shiri, "Estimation of reference evapotranspiration using spatial and temporal machine learning approaches," *Hydrology*, vol. 8, no. 1, p. 25, Feb. 2021. [Online]. Available: <https://www.mdpi.com/2306-5338/8/1/25/>.
- [27] Y. Feng, N. Cui, D. Gong, Q. Zhang, and L. Zhao, "Evaluation of random forests and generalized regression neural networks for daily reference evapotranspiration modelling," *Agricult. Water Manage.*, vol. 193, pp. 163–173, Nov. 2017.
- [28] A. Fernández-López, D. Marín-Sánchez, G. García-Mateos, A. Ruiz-Canales, M. Ferrández-Villena-García, and J. M. Molina-Martínez, "A machine learning method to estimate reference evapotranspiration using soil moisture sensors," *Appl. Sci.*, vol. 10, no. 6, p. 1912, Mar. 2020.
- [29] F. Granata, "Evapotranspiration evaluation models based on machine learning algorithms—A comparative study," *Agricult. Water Manage.*, vol. 217, pp. 303–315, May 2019.
- [30] R. S. Krishnan, E. G. Julie, Y. H. Robinson, S. Raja, R. Kumar, P. H. Thong, and L. H. Son, "Fuzzy logic based smart irrigation system using Internet of Things," *J. Cleaner Prod.*, vol. 252, Apr. 2020, Art. no. 119902.
- [31] S. Aggarwal and A. Kumar, "A smart irrigation system to automate irrigation process using IoT and artificial neural network," in *Proc. 2nd Int. Conf. Signal Process. Commun. (ICSPC)*, Mar. 2019, pp. 310–314.
- [32] B. Petković, D. Petković, B. Kuzman, M. Milovančević, K. Wakil, L. S. Ho, and K. Jermittiparsert, "Neuro-fuzzy estimation of reference crop evapotranspiration by neuro fuzzy logic based on weather conditions," *Comput. Electron. Agricult.*, vol. 173, Jun. 2020, Art. no. 105358.
- [33] S. Koduru, V. P. R. Padala, and P. Padala, "Smart irrigation system using cloud and Internet of Things," in *Proc. 2nd Int. Conf. Commun., Comput. Netw.* Singapore: Springer, 2019, pp. 195–203.
- [34] Y. Feng, Y. Peng, N. Cui, D. Gong, and K. Zhang, "Modeling reference evapotranspiration using extreme learning machine and generalized regression neural network only with temperature data," *Comput. Electron. Agricult.*, vol. 136, pp. 71–78, Apr. 2017.
- [35] C. M. Angelopoulos, G. Filios, S. Nikolettseas, and T. P. Raptis, "Keeping data at the edge of smart irrigation networks: A case study in strawberry greenhouses," *Comput. Netw.*, vol. 167, Feb. 2020, Art. no. 107039.
- [36] N. G. S. Campos, A. R. Rocha, R. Gondim, T. L. C. da Silva, and D. G. Gomes, "Smart & green: An internet-of-things framework for smart irrigation," *Sensors*, vol. 20, no. 1, p. 190, 2020.
- [37] N. K. Nawandar and V. R. Satpute, "IoT based low cost and intelligent module for smart irrigation system," *Comput. Electron. Agricult.*, vol. 162, pp. 979–990, Jul. 2019.
- [38] P. Fraga-Lamas, M. Celaya-Echarri, L. Azpilicueta, P. Lopez-Iturri, F. Falcone, and T. M. Fernández-Caramés, "Design and empirical validation of a LoRaWAN IoT smart irrigation system," *Proceedings*, vol. 42, no. 1, p. 62, 2020.
- [39] A. Anitha, N. Sampath, and M. A. Jerlin, "Smart irrigation system using Internet of Things," in *Proc. Int. Conf. Emerg. Trends Inf. Technol. Eng. (ic-ETITE)*, Feb. 2020, pp. 96–101.
- [40] J. Shi, X. Wu, M. Zhang, X. Wang, Q. Zuo, X. Wu, H. Zhang, and A. Ben-Gal, "Numerically scheduling plant water deficit index-based smart irrigation to optimize crop yield and water use efficiency," *Agricult. Water Manage.*, vol. 248, Apr. 2021, Art. no. 106774.
- [41] G. Singh, D. Sharma, A. Goap, S. Sehgal, A. K. Shukla, and S. Kumar, "Machine learning based soil moisture prediction for Internet of Things based smart irrigation system," in *Proc. 5th Int. Conf. Signal Process., Comput. Control (ISPCC)*, Oct. 2019, pp. 175–180.
- [42] R. Togneri, C. Kamienski, R. Dantas, R. Prati, A. Toscano, J.-P. Soininen, and T. S. Cinotti, "Advancing IoT-based smart irrigation," *IEEE Internet Things Mag.*, vol. 2, no. 4, pp. 20–25, Dec. 2019.
- [43] D. Thakur, Y. Kumar, and S. Vijendra, "Smart irrigation and intrusions detection in agricultural fields using I.o.T.," *Proc. Comput. Sci.*, vol. 167, pp. 154–162, Jan. 2020.
- [44] N. M. Tiglaio, M. Alipio, J. V. Balanay, E. Saldivar, and J. L. Tiston, "Agrinex: A low-cost wireless mesh-based smart irrigation system," *Measurement*, vol. 161, Sep. 2020, Art. no. 107874.
- [45] A. Dasgupta, A. Daruka, A. Pandey, A. Bose, S. Mukherjee, and S. Saha, "Smart irrigation: IoT-based irrigation monitoring system," in *Proceedings of International Ethical Hacking Conference 2018*. Singapore: Springer, 2019, pp. 395–403.
- [46] S. Akshay and T. K. Ramesh, "Efficient machine learning algorithm for smart irrigation," in *Proc. Int. Conf. Commun. Signal Process. (ICCS)*, Jul. 2020, pp. 867–870.
- [47] R. Liao, S. Zhang, X. Zhang, M. Wang, H. Wu, and L. Zhangzhong, "Development of smart irrigation systems based on real-time soil moisture data in a greenhouse: Proof of concept," *Agricult. Water Manage.*, vol. 245, Feb. 2021, Art. no. 106632.
- [48] K. E. Lakshmi Prabha and C. Govindaraju, "Hydroponic-based smart irrigation system using Internet of Things," *Int. J. Commun. Syst.*, p. e4071, Jul. 2019.
- [49] *Chapter 2—FAO Penman-Monteith Equation*, FAO, Rome, Italy, 2017.

...